Accepted in M3AS

Evaluation of Flux Integral Outputs for the Reduced Basis Method

Jens L. Eftang*and Einar M. Rønquist†

20th October 2009

Abstract

In this paper, we consider the evaluation of flux integral outputs from reduced basis solutions to second-order PDE's. In order to evaluate such outputs, a lifting function $v^\star$ must be chosen. In the standard finite element context, this choice is not relevant, whereas in the reduced basis context, as we show, it greatly affects the output error. We propose two "good" choices for $v^\star$, and illustrate their effect on the output error by examining a numerical example. We also make clear the role of $v^\star$ in a more general primal-dual reduced basis approximation framework.

1 Introduction

For many practical applications, one is interested in certain physical averages, or *outputs of interest*, which can be defined as functionals of the solution to a partial differential equation (PDE) that describes an underlying physical problem. For example, the output of interest may be the average heat flux through (or average temperature on) a surface, or the average force acting on a wall due to fluid flow. In this paper, we are concerned with outputs of *flux integral type*, i.e., outputs that can be written as surface integrals of the normal derivative of the solution to the underlying PDE. We consider second-order equations, for which it is possible to evaluate flux integral outputs directly via the weak problem formulation, and in particular without the need for any numerical differentiation.

Mathematically, we consider a weakly written problem defined on a domain Ω: Find $u \in X(\Omega)$ such that

$$a(u, v) = f(v), \quad \forall v \in X(\Omega), \tag{1}$$

where a is a coercive, continuous and for simplicity also symmetric bilinear form derived from some second-order differential operator, f is a linear and bounded

*Department of Mathematical Sciences, Norwegian University of Science and Technology, 7491 Trondheim, Norway, eftang@math.ntnu.no

†Department of Mathematical Sciences, Norwegian University of Science and Technology, 7491 Trondheim, Norway, ronquist@math.ntnu.no

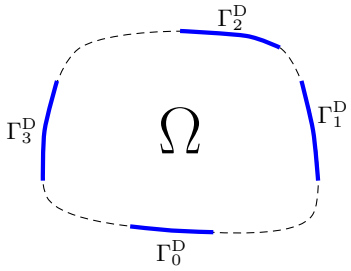

Figure 1: Illustration of a general domain Ω in the particular case that the Dirichlet boundary $\Gamma^{\mathrm{D}} = \cup_{k=0}^{K-1}\Gamma_k^{\mathrm{D}}$ consists of $K = 4$ disjoint sections.

functional, $X(\Omega) = \{v \in H^1(\Omega) : v|_{\Gamma^{\mathrm{D}}} = 0\}$ is our exact space, and $\Gamma^{\mathrm{D}} \subset \partial\Omega$ denotes the parts of the boundary of Ω on which we impose (for simplicity homogeneous) Dirichlet boundary conditions. As usual, $H^1(\Omega)$ denotes the Sobolev space of functions with square integrable first order derivatives. Henceforth, the Ω-dependence of our spaces is understood when no ambiguity may arise.

We shall assume that the Dirichlet boundary, Γ^{D}, may be written as $\Gamma^{\mathrm{D}} = \cup_{k=0}^{K-1}\Gamma_k^{\mathrm{D}}$, where $\Gamma_k^{\mathrm{D}} \subset \partial\Omega$, $0 \leq k \leq K-1$, are disjoint sections, as illustrated in Figure 1 for the special case $K = 4$. In addition, we require any two such sections Γ_i^{D} and Γ_j^{D} $(i \neq j)$ to be separated by a section on which a Neumann boundary condition is imposed. Our output of interest shall be the integral of the flux through $\Gamma_0^{\mathrm{D}} \subseteq \Gamma^{\mathrm{D}}$, i.e., the integral of the flux through an entire separate section of Γ^{D}. We thus define the output functional

$$\tilde{l}^{\mathrm{out}}(w) \equiv \int_{\Gamma_0^{\mathrm{D}}} \frac{\partial w}{\partial n}\,\mathrm{d}s, \tag{2}$$

where $\partial/\partial n$ denotes the outward normal derivative and s is the surface measure on $\partial\Omega$. When solving e.g. Poisson or Helmholtz problems with the finite element (FE) method, it is preferable [1, 2, 6, 10] to instead evaluate flux integral outputs through an affine functional

$$l^{\mathrm{out}}(w) \equiv a(w, v^\star) - f(v^\star), \tag{3}$$

where $v^\star \in H^1$ is any function that is equal to unity on Γ_0^{D} and equal to zero on $\Gamma^{\mathrm{D}} \setminus \Gamma_0^{\mathrm{D}}$. Of course, even though (2) and (3) make sense for any $w \in X$, they are only of interest for $w \approx u$, where u is the solution of (1). One way to derive (3), is to recast the original problem (1) as a "Neumann problem" for which there are no restrictions on the test and trial functions on Γ_0^{D}. Thus, if we suppose (1) is a Poisson or Helmholtz problem, this modified problem reads: Find $u \in \tilde{X}$ such that

$$a(u, v) = f(v) + \int_{\Gamma_0^{\mathrm{D}}} \frac{\partial u}{\partial n} v\,\mathrm{d}s, \quad \forall v \in \tilde{X}, \tag{4}$$

where $\tilde{X} = \{v \in H^1 : v|_{\Gamma^{\mathrm{D}} \setminus \Gamma_0^{\mathrm{D}}} = 0\} \supset X$. Moving $f(v)$ to the left hand side and choosing $v = v^\star \in \tilde{X}$, we see that $\tilde{l}^{\mathrm{out}}(u) = l^{\mathrm{out}}(u)$.

Suppose we solve (1) numerically to obtain a FE approximation to u, $u^{\mathcal{N}} \in X^{\mathcal{N}}$, satisfying

$$a(u^{\mathcal{N}}, v) = f(v), \quad \forall v \in X^{\mathcal{N}}. \tag{5}$$

Here, $X^{\mathcal{N}} \subset X$ is a discrete FE space with $\mathcal{N}$ degrees of freedom. The FE output of interest can now be evaluated in two ways, either as $\tilde{l}^{\mathrm{out}}(u^{\mathcal{N}})$ or as $l^{\mathrm{out}}(u^{\mathcal{N}})$. In the latter case, we substitute $u^{\mathcal{N}}$ for u and consequently $\approx$ for $=$ in (4). With $v = v^\star$, we get $l^{\mathrm{out}}(u^{\mathcal{N}}) \approx \int_{\Gamma_0^{\mathrm{D}}} \frac{\partial u^{\mathcal{N}}}{\partial n} \, \mathrm{d}s$. Hence, in general, $l^{\mathrm{out}}(u^{\mathcal{N}}) \neq \tilde{l}^{\mathrm{out}}(u^{\mathcal{N}})$.

We shall refer to $v^\star$ as a *flux lifting function*, and we shall denote the set of possible such functions as $V^\star$. Specifically,

$$V^\star \equiv \{v \in H^1 : v|_{\Gamma^{\mathrm{D}} \setminus \Gamma_0^{\mathrm{D}}} = 0, v|_{\Gamma_0^{\mathrm{D}}} = 1\}. \tag{6}$$

In [2], $v^\star$ is called an *extraction function*, and the method described above for flux integral output evaluation is an example of an *extraction method*. In [10], the method – with more emphasis on pointwise quantities, rather than on surface integrals – is called *the consistent Galerkin FEM*. A collection of *post-processing methods* for flux integral and other types of outputs, including pointwise quantities, can be found in [1]. In any event, $l^{\mathrm{out}}(u^{\mathcal{N}})$ typically converges to $l^{\mathrm{out}}(u)$ quadratically with the energy-norm error of the field variable, $\|u - u^{\mathcal{N}}\|$, in contrast to $\tilde{l}^{\mathrm{out}}(u^{\mathcal{N}})$, which typically exhibits only linear convergence [2, 6]. Another advantage of l^{out} over $\tilde{l}^{\mathrm{out}}$ is that the former requires no calculation of normal derivatives, which is particularly convenient in higher dimensions and for problems on domains with curved boundaries.

Aside from the essential boundary condition in (6), we have not made any particular choice for $v^\star \in H^1$. In fact, within a standard finite element framework, this choice is not a big issue due to Galerkin orthogonality and the richness of the approximation spaces used [2, 6]. (It is, however, important that $v^\star$ be a smooth function on each element [1].) In contrast, as we will show numerically and theoretically, one should take a little more care when evaluating flux integral outputs by way of the method described above within the *reduced basis* (RB) framework. For a thorough introduction to RB methods, confer e.g. [19].

In the next section, we shall consider a very simple numerical example which illustrates how l^{out} may be superior to $\tilde{l}^{\mathrm{out}}$ in terms of numerical accuracy within the FE framework. In Section 3, we first briefly review the RB method and then elaborate on the discrepancy between the FE and RB methods with respect to the choice of $v^\star$. We then propose two "good" choices for $v^\star$ to use in the RB context. We also make clear the role of $v^\star$ in the more general primal-dual RB approximation procedure that is used to speed up the convergence for non-compliant problems [17, 19] In Section 4, we remain in the RB context and illustrate the effect of different $v^\star$'s by examining yet another numerical example, and in Section 5 we end our discussion with some concluding remarks.

2 Flux Output Evaluation: a 1D Example

We consider a one-dimensional Helmholtz problem on $\Omega = (0, 2)$ with homogeneous Dirichlet boundary conditions. The weak formulation of the problem reads: Find $u \in H^1_0$ such that

$$\underbrace{\int_0^2 \left(\frac{\partial u}{\partial x} \frac{\partial v}{\partial x} + uv \right) \mathrm{d}x}_{=a(u,v)} = \underbrace{\int_0^2 qv \, \mathrm{d}x}_{=f(v)}, \quad \forall v \in H^1_0, \tag{7}$$

where $H^1_0 = \{v \in H^1 : v(0) = v(2) = 0\}$. For the purpose of this example, we want the solution u to be weakly singular. In order to achieve this, we choose the source term as $q(x) = x^{2/3}$. Our output of interest is the derivative of u at $x = \Gamma^{\mathrm{D}}_0 = \{2\}$, and our two output functionals now reduce to

$$\tilde{l}^{\mathrm{out}}(w) = \left. \frac{\partial w}{\partial x} \right|_{x=2} \tag{8}$$

and

$$l^{\mathrm{out}}(w) = a(w, v^\star) - f(v^\star), \tag{9}$$

where $v^\star \in V^\star$.

With a spectral (high order polynomial) method, we discretise (7) and find $u^{\mathcal{N}} \in X^{\mathcal{N}}$ such that

$$a(u^{\mathcal{N}}, v) = f(v), \quad \forall v \in X^{\mathcal{N}}, \tag{10}$$

where

$$X^{\mathcal{N}} = \{v \in \mathbb{P}_{\mathcal{N}} : v_{\Gamma^{\mathrm{D}}} = 0\} \tag{11}$$

is our discrete space. Here, $\Gamma^{\mathrm{D}} = \{0, 2\}$ and $\mathbb{P}_{\mathcal{N}}$ denotes the space of polynomials of degree $\mathcal{N}$ (note that here, $\dim(X^{\mathcal{N}}) = \mathcal{N} - 1$ due to the Dirichlet boundary conditions).

We shall also consider the dual problem: Find $\psi \in H^1_0$ such that

$$a(v, \psi) = -a(v, v^\star), \quad \forall v \in H^1_0. \tag{12}$$

The spectral discretisation of (12) reads: Find $\psi^{\mathcal{N}} \in X^{\mathcal{N}}$ such that

$$a(v, \psi^{\mathcal{N}}) = -a(v, v^\star), \quad \forall v \in X^{\mathcal{N}}. \tag{13}$$

Note that $a(v, v^\star)$ – the (bounded) linear functional part of l^{out} – enters on the right hand side in the dual problem (with a minus sign). Thus, $v^\star$ also plays the role of a Dirichlet lifting function for the dual problem, with Dirichlet data equal to unity on Γ^{D}_0 (i.e. at $x = 2$). Also note that the dual problem exhibits no (singular) source term. Provided $v^\star$ is smooth (deliberately choosing $v^\star$ singular

seems somewhat peculiar), we expect ψ to be a smooth function and thus the convergence of $\psi^{\mathcal{N}}$ to ψ to be of infinite order.

We are interested in the errors in the output of interest, which we define for each of our two output functionals as

$$\tilde{e}^{\mathcal{N},\text{out}} \equiv \left| \frac{\partial u}{\partial x}\Big|_{x=2} - \tilde{l}^{\text{out}}(u^{\mathcal{N}}) \right|, \tag{14}$$

and

$$e^{\mathcal{N},\text{out}} \equiv \left| \frac{\partial u}{\partial x}\Big|_{x=2} - l^{\text{out}}(u^{\mathcal{N}}) \right| = \left| l^{\text{out}}(u) - l^{\text{out}}(u^{\mathcal{N}}) \right|, \tag{15}$$

respectively. For $e^{\mathcal{N},\text{out}}$, we deduce that

$$\begin{aligned} e^{\mathcal{N},\text{out}} &= |a(u - u^{\mathcal{N}}, v^\star)| \\ &= |a(u - u^{\mathcal{N}}, \psi)| \\ &= |a(u - u^{\mathcal{N}}, \psi - \psi^{\mathcal{N}})| \\ &\le \|u - u^{\mathcal{N}}\| \|\psi - \psi^{\mathcal{N}}\|, \end{aligned} \tag{16}$$

by using the definition of $e^{\mathcal{N},\text{out}}$, the fact that $u^{\mathcal{N}} - u \in H_0^1$ and the definition of the dual problem (12), Galerkin orthogonality of $u - u^{\mathcal{N}}$ and the Cauchy-Schwarz inequality, respectively. Here, $\|\cdot\| = \sqrt{a(\cdot,\cdot)}$ denotes the energy norm. A consequence of this estimate is that if ψ happens to be a smooth function, $e^{\mathcal{N},\text{out}}$ will decay exponentially with $\mathcal{N}$, even if u is singular. Note that in practice, we never actually compute the discrete solution $\psi^{\mathcal{N}}$ to the dual problem.

In Figure 2, we plot the energy norm error $\|u - u^{\mathcal{N}}\|$ and the output errors $\tilde{e}^{\mathcal{N},\text{out}}$ and $e^{\mathcal{N},\text{out}}$ for $1 \le \mathcal{N} \le 50$. As our flux lifting function, we have made the choice $v^\star = x/2$. As expected, the error $\|u - u^{\mathcal{N}}\|$ decays algebraically, while $e^{\mathcal{N},\text{out}}$ decays at an infinite rate due to the smoothness of ψ. Note that we reach double precision accuracy for $e^{\mathcal{N},\text{out}}$ for $\mathcal{N} \gtrsim 10$.

Let us make a few remarks concerning the above results. Firstly, although for $v, w \in X^{\mathcal{N}}$ the integrals $a(v,w)$ and $f(v)$ are easy to evaluate analytically, we have chosen to perform all integration by using numerical quadrature since we can then employ a very general computational framework (which can also be used to solve more difficult problems in which analytic integration is not possible). However, since $q(x) = x^{2/3}$ is not a smooth function over Ω, the integrand on the right hand side of the primal problem is singular, and hence accurate evaluation of the integral $f(v)$ requires quadrature of very high order. If $f(v)$ is not computed with sufficient accuracy, $u^{\mathcal{N}}$ will carry an additional numerical integration error which will compromise Galerkin orthogonality – which we exploited in the error bound (16) – and hence also the exponential convergence of the output. In our numerical experiment, we assume negligible numerical integration errors since all numerical integration is performed with Gauss-Lobatto-Legendre (GLL) quadrature [5] over $n_q \gg \mathcal{N} + 1$ quadrature points. Specifically, $n_q = 121$.

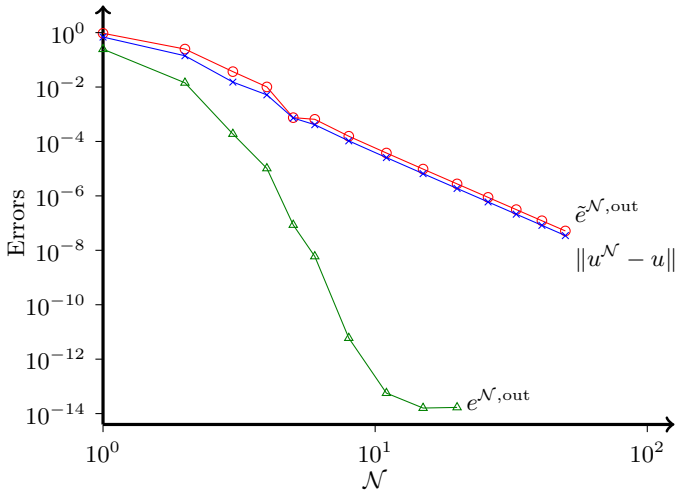

Figure 2: Energy error ($\times$) and output errors $e^{\mathcal{N},\text{out}}$ ($\triangle$) and $\tilde{e}^{\mathcal{N},\text{out}}$ ($\circ$) for increasing polynomial degree, $\mathcal{N}$, of the underlying spectral approximation.

Secondly, we note that the error $\|u - u^{\mathcal{N}}\|$ decays much faster than expected from the standard error estimate. It can be shown that, for our problem, the most singular term of u behaves like $x^{8/3}$, and hence $u \in H^{\sigma}$ for all $0 \leq \sigma < 19/6$. From the standard estimate [5], we would expect $\|u - u^{\mathcal{N}}\| \leq c\mathcal{N}^{1-\sigma}$ for some positive constant c, and hence a slope of $-13/6$. In contrast, the actual decay is in fact of order -4.33, which is twice as good as expected. The reason for this superconvergence is related to the particular type of singularity exhibited by the solution to our problem – it appears at an endpoint and is of x^{α}-type – and the rather good capability of polynomials to approximate functions with such singularities [4, 12].

Thirdly, we note that for our simple one-dimensional problem, $\tilde{e}^{\mathcal{N},\text{out}}$ decays as fast as the error $\|u - u^{\mathcal{N}}\|$. We would expect similar results were we to use a linear (h-type) finite element method. In fact, if u_h denotes a linear FE approximation to u on a mesh with elements of size h, we would from standard FE error estimates [18] expect convergence of order $\mathcal{O}(h^2)$ for the output $l^{\text{out}}(u_h)$, and of order $\mathcal{O}(h)$ for the energy-norm error $\|u - u_h\|$ (note that for our particular problem, the singularity in u is weak enough that full linear convergence (in h) is achieved). Based on the preceeding results, we would also expect convergence of order $\mathcal{O}(h)$ for the output $\tilde{l}^{\text{out}}(u_h)$. Indeed, our results and comments here are consistent with results presented in [6] and a note made in [2] for the h and and h-p finite element methods, respectively, applied to the problem (10).

Finally, as noted in [2], any two choices of $v^{\star} \in (V^{\star} \cap \tilde{X}^{\mathcal{N}})$ produce the same result for $l^{\text{out}}(u^{\mathcal{N}})$. To see this, let $v_1^{\star}, v_2^{\star} \in (V^{\star} \cap \tilde{X}^{\mathcal{N}})$. Then $w^{\star} = v_1^{\star} - v_2^{\star} \in$

$X^{\mathcal{N}}$, and

$$\left[a(u^{\mathcal{N}}, v_1^\star) - l(v_1^\star)\right] - \left[a(u^{\mathcal{N}}, v_2^\star) - l(v_2^\star)\right] = a(u^{\mathcal{N}}, w^\star) - l(w^\star) = 0, \quad (17)$$

by (10). A convenient choice for $v^\star$, then, is the function that is equal to unity at the node at $x = 2$ and equal to zero at every other node (or, in the low-order finite element case, the function that is equal to unity at $x = 2$ with support only on the element adjacent to the boundary). For this reason, we do not specifically emphasise our choice for $v^\star$ when considering outputs from FE solutions.

In the next section, we turn our focus to flux integral outputs in the reduced basis context.

3 Flux Output Evaluation within the Reduced Basis Framework

3.1 Reduced basis formulation

3.1.1 Parameterised weak form

Of interest within the reduced basis (RB) framework [9, 17, 19] is the solution – and ultimately the corresponding output of interest – of parameter-dependent PDE's in cases where the output is either required in real time, or for a large number of input parameters. In the following, $\mathcal{D} \subset \mathbb{R}^P$ shall denote the admissible parameter domain, and $\boldsymbol{\mu} \in \mathcal{D}$ a parameter P-tuple that governs e.g. boundary conditions or material or geometrical properties of the underlying physical problem. We shall consider the following parameterised problem on a domain Ω: Given any $\boldsymbol{\mu} \in \mathcal{D}$, find $u(\boldsymbol{\mu}) \in X$ such that

$$a(u(\boldsymbol{\mu}), v; \boldsymbol{\mu}) = f(v; \boldsymbol{\mu}), \quad \forall v \in X, \quad (18)$$

where, for each $\boldsymbol{\mu} \in \mathcal{D}$, $a(\cdot, \cdot; \boldsymbol{\mu})$ is a coercive, continuous and for simplicity also symmetric bilinear form originating from a second-order differential operator, and $f(\cdot; \boldsymbol{\mu})$ is a linear and bounded functional. We also assume that a and f are parametrically affine, in the sense that the $\boldsymbol{\mu}$-dependency of a and f take the form

$$a(v, w; \boldsymbol{\mu}) = \sum_{q=1}^{Q_a} a^q(v, w)\Theta_a^q(\boldsymbol{\mu}), \quad f(v; \boldsymbol{\mu}) = \sum_{q=1}^{Q_f} f^q(v)\Theta_f^q(\boldsymbol{\mu}), \quad (19)$$

for finite numbers Q_a and Q_f, where the a^q and f^q are parameter independent bilinear and linear forms, respectively, and the Θ_a^q and Θ_f^q are parameter dependent functions.

We still impose homogeneous Dirichlet boundary conditions on $\Gamma^{\mathrm{D}} \subset \partial\Omega$, and take as our exact output of interest the flux integral

$$\tilde{s}(\boldsymbol{\mu}) = \int_{\Gamma_0^{\mathrm{D}}} \frac{\partial u(\boldsymbol{\mu})}{\partial n} \, \mathrm{d}s, \quad (20)$$

where $\Gamma_0^{\mathrm{D}} \subseteq \Gamma^{\mathrm{D}}$ is an entire separate section of the Dirichlet boundary.

Finally, we define the now parameter dependent "energy" norm

$$\|\cdot\|_{\boldsymbol{\mu}} \equiv \sqrt{a(\cdot,\cdot;\boldsymbol{\mu})}, \tag{21}$$

and the equivalent parameter-independent X-norm

$$\|\cdot\|_X \equiv \sqrt{a(\cdot,\cdot;\bar{\boldsymbol{\mu}})}, \tag{22}$$

where $\bar{\boldsymbol{\mu}} \in \mathcal{D}$ is some fixed, preselected reference parameter. Note that by the assumptions of symmetry, coercivity and continuity, $a(\cdot,\cdot;\boldsymbol{\mu})$ defines an inner-product, and $\|\cdot\|_{\boldsymbol{\mu}}$ a norm equivalent to the H_1-norm, for each $\boldsymbol{\mu} \in \mathcal{D}$.

3.1.2 FE "truth" approximation

The reduced basis approximations will be built upon snapshots of "truth" finite element approximations to solutions of (18), computed for wisely selected points in the admissible parameter domain. Let $X^{\mathcal{N}}$ be a standard finite element discrete space with $\mathcal{N}$ degrees of freedom. The "truth" discretisation of (18) reads: For any $\boldsymbol{\mu} \in \mathcal{D}$, find $u^{\mathcal{N}}(\boldsymbol{\mu}) \in X^{\mathcal{N}}$ such that

$$a(u^{\mathcal{N}}(\boldsymbol{\mu}), v; \boldsymbol{\mu}) = f(v;\boldsymbol{\mu}), \quad \forall v \in X^{\mathcal{N}}. \tag{23}$$

The corresponding "truth" output of interest is

$$s^{\mathcal{N}}(\boldsymbol{\mu}) \equiv l^{\mathrm{out}}(u^{\mathcal{N}}(\boldsymbol{\mu});\boldsymbol{\mu}) \equiv a(u^{\mathcal{N}}(\boldsymbol{\mu}), v^\star;\boldsymbol{\mu}) - f(v^\star;\boldsymbol{\mu}). \tag{24}$$

By the appellation "truth", we here understand that, for all $\boldsymbol{\mu} \in \mathcal{D}$, the FE solution and output errors are assumed smaller than some prescribed (problem dependent) tolerance. Moreover, for any given $\boldsymbol{\mu} \in \mathcal{D}$, the RB *a posteriori* error estimators (to which we return in Section 3.3) provide upper bounds only for the gap between the RB field, or output, and the corresponding "truth" FE field, or output, respectively. Hence, the RB fields and outputs are both built upon and estimated relative to the "truth" fields and outputs, respectively, which thus in effect serve as surrogates for the exact fields and outputs, respectively.

3.1.3 RB approximation

For $1 \le N \le N_{\max}$, the RB approximation space, X_N, will be the span of precomputed snapshots taken of $u^{\mathcal{N}}$ at N different points in $\mathcal{D}$. Specifically, given a set of N wisely selected parameter vectors $\boldsymbol{\mu}_1, \boldsymbol{\mu}_2, \ldots, \boldsymbol{\mu}_N \in \mathcal{D}$, we define the corresponding RB space as

$$X_N = \mathrm{span}\{u^{\mathcal{N}}(\boldsymbol{\mu}_1), \ldots, u^{\mathcal{N}}(\boldsymbol{\mu}_N)\}. \tag{25}$$

We assume the $u^{\mathcal{N}}(\boldsymbol{\mu}_n)$, $1 \le n \le N$, to be linearly independent. The reduced basis problem now becomes: Given any $\boldsymbol{\mu} \in \mathcal{D}$, find $u_N(\boldsymbol{\mu}) \in X_N$ such that

$$a(u_N(\boldsymbol{\mu}), v; \boldsymbol{\mu}) = f(v;\boldsymbol{\mu}), \quad \forall v \in X_N, \tag{26}$$

and evaluate the RB flux integral output

$$s_N(\boldsymbol{\mu}) \equiv l^{\text{out}}(u_N(\boldsymbol{\mu}); \boldsymbol{\mu}) = a(u_N(\boldsymbol{\mu}), v^\star; \boldsymbol{\mu}) - f(v^\star; \boldsymbol{\mu}). \tag{27}$$

Starting from an initial (e.g. randomly chosen) $\boldsymbol{\mu}_1 \in \mathcal{D}$, the parameter vectors $\boldsymbol{\mu}_N$, $2 \leq N \leq N_{\max}$, are chosen one at a time in a greedy manner. For each value of N, we evaluate the *a posteriori* (e.g. field energy norm) error estimator, $\Delta_{N-1}(\boldsymbol{\mu})$, for every $\boldsymbol{\mu}$ in a finite training sample, $\Xi_{\text{train}} \subset \mathcal{D}$. We then choose $\boldsymbol{\mu}_N$ equal to $\boldsymbol{\mu} \in \Xi_{\text{train}}$ that maximises $\Delta_{N-1}(\boldsymbol{\mu})$, and compute the corresponding snapshot $u^{\mathcal{N}}(\boldsymbol{\mu}_N)$ as the next RB basis function. The greedy parameter selection procedure was introduced in [21]. For a detailed description, see also [19].

Note that we have assumed evaluation of the "truth" and RB flux integral outputs in (24) and (27), respectively, by using a flux lifting function $v^\star \in V^\star$, although we have not yet made any particular choice for $v^\star$.

Under the assumption that $u^{\mathcal{N}}(\boldsymbol{\mu})$ varies smoothly with $\boldsymbol{\mu} \in \mathcal{D}$, we may expect that – for any $\boldsymbol{\mu} \in \mathcal{D}$ – very few RB basis functions will suffice in order to reproduce a very good RB approximation, $u_N(\boldsymbol{\mu})$, to the corresponding "truth" approximation, $u^{\mathcal{N}}(\boldsymbol{\mu})$, via the Galerkin formulation (26). Consequently, the corresponding RB output, $s_N(\boldsymbol{\mu})$, will be very close to the "truth" output, $s^{\mathcal{N}}(\boldsymbol{\mu})$. In particular, for a fixed level of accuracy relative to the *exact* field, $u(\boldsymbol{\mu})$, or output, $\tilde{s}(\boldsymbol{\mu})$, we expect that the number of required degrees of freedom associated with the RB approximations, N, is much lower than the number of required degrees of freedom associated with the "truth" approximations, $\mathcal{N}$, since the RB approximation space is specifically taylored to the problem at hand. As a result, only a small system of algebraic equations needs to be solved for each new given $\boldsymbol{\mu}$, once a sufficiently large RB space, X_N, is constructed.

Imperative to the efficiency of the RB method is a computational decoupling in offline (preprocessing) and online stages. The offline stage – which is performed only once – may be computationally very costly and includes the greedy parameter selection process and the computation of the corresponding "truth" snapshots, i.e., the RB basis functions. The online stage – in which, given any new $\boldsymbol{\mu} \in \mathcal{D}$, the RB solution, $u_N(\boldsymbol{\mu})$, and RB output of interest, $s_N(\boldsymbol{\mu})$, are computed – is very fast. In particular, owing to the assumptions (19) on parametric affinity, the computational complexity of the RB online stage can be made independent of $\mathcal{N}$ [19].

Of interest within the RB context is the concept of a *compliant* problem. A problem is said to be compliant if, for all $\boldsymbol{\mu} \in \mathcal{D}$, *i)* the output functional $l^{\text{out}}(\cdot; \boldsymbol{\mu})$ (more generally, in the case of $l^{\text{out}}(\cdot; \boldsymbol{\mu})$ affine, the linear functional part of $l^{\text{out}}(\cdot; \boldsymbol{\mu})$) is equal to the right-hand-side $f(\cdot; \boldsymbol{\mu})$ of (18), and *ii)* $a(\cdot, \cdot; \boldsymbol{\mu})$ is symmetric. In the compliant case, the error in the RB output of interest is *equal* to the square of the energy-norm error of the primary field variable [17, 19].

In our case, $l^{\text{out}}(\cdot; \boldsymbol{\mu})$ as defined in (24) (or (27)) above is a non-compliant output functional since its linear functional part $a(\cdot, v^\star; \boldsymbol{\mu})$ is, in general, different from the right-hand-side $f(\cdot; \boldsymbol{\mu})$ of (18), and that it is, strictly speaking, not

linear, but affine, due to the translation term $f(v^\star;\boldsymbol{\mu})$. We make a comment in Section 4.4 on a very particular case in which $l^{\text{out}}(\cdot;\boldsymbol{\mu})$ is, in fact, compliant.

3.2 Relevance of the flux lifting function

In Section 2, we saw that any two choices for $v^\star$ belonging to $(V^\star \cap \tilde{X}^{\mathcal{N}})$ produced the same output $l^{\text{out}}(u^{\mathcal{N}})$ within a standard FE framework. This is of course a consequence of Galerkin orthogonality and, when compared to the RB space, X_N, the richness and generality of the FE space, $X^{\mathcal{N}}$. Within the RB framework however, the choice of flux lifting function does affect the numerical value of the output. To see this, let $v_1^\star, v_2^\star \in (V^\star \cap \tilde{X}^{\mathcal{N}})$, and define $w^\star \equiv v_1^\star - v_2^\star$. In order to denote the RB output for a particular $\boldsymbol{\mu} \in \mathcal{D}$, computed with a particular $v^\star$, we write

$$s_N(\boldsymbol{\mu}; v^\star) \equiv a(u_N(\boldsymbol{\mu}), v^\star; \boldsymbol{\mu}) - f(v^\star; \boldsymbol{\mu}). \tag{28}$$

Hence, the outputs corresponding to $v_1^\star$ and $v_2^\star$ are given by

$$s_N(\boldsymbol{\mu}; v_1^\star) = a(u_N(\boldsymbol{\mu}), v_1^\star; \boldsymbol{\mu}) - f(v_1^\star; \boldsymbol{\mu}), \tag{29}$$
$$s_N(\boldsymbol{\mu}; v_2^\star) = a(u_N(\boldsymbol{\mu}), v_2^\star; \boldsymbol{\mu}) - f(v_2^\star; \boldsymbol{\mu}), \tag{30}$$

respectively. But then,

$$\begin{aligned} s_N(\boldsymbol{\mu}; v_1^\star) - s_N(\boldsymbol{\mu}; v_2^\star) &= a(u_N(\boldsymbol{\mu}), v_1^\star; \boldsymbol{\mu}) - f(v_1^\star; \boldsymbol{\mu}) \\ &\quad - \big(a(u_N(\boldsymbol{\mu}), v_2^\star; \boldsymbol{\mu}) - f(v_2^\star; \boldsymbol{\mu})\big) \\ &= a(u_N(\boldsymbol{\mu}), w^\star; \boldsymbol{\mu}) - f(w^\star; \boldsymbol{\mu}), \end{aligned} \tag{31}$$

which by (26) is equal to zero for all $w^\star \in X_N$. However, there must clearly exist $w^\star \in X^{\mathcal{N}}$ such that $a(u_N(\boldsymbol{\mu}), w^\star; \boldsymbol{\mu}) - f(w^\star; \boldsymbol{\mu})$ is *nonzero*. Otherwise, $u_N(\boldsymbol{\mu})$ would have been identical to $u^{\mathcal{N}}(\boldsymbol{\mu})$, which is provably not the case for a general $\boldsymbol{\mu} \in \mathcal{D}$. In conclusion, the two evaluations $s_N(\boldsymbol{\mu}, v_1^\star)$ and $s_N(\boldsymbol{\mu}, v_2^\star)$ are not in general equivalent (unless $v_1^\star - v_2^\star$ happens to belong to X_N). Naturally, this raises the question of which $v^\star$ we should choose within the RB framework.

3.3 *A posteriori* error estimation

Before we proceed to our actual choices for "good" RB flux lifting functions, we shall consider the *a posteriori* error upper bound associated with the output $s_N(\boldsymbol{\mu})$. To arrive at such a bound, we first require a bound for the error in the field variable. We assume that we have available a lower bound $\alpha_{\text{LB}}(\boldsymbol{\mu}) > 0$ for the coercivity constant of $a(\cdot, \cdot; \boldsymbol{\mu})$ over $X^{\mathcal{N}}$ with respect to the X-norm defined in (22). Specifically, for all $\boldsymbol{\mu} \in \mathcal{D}$,

$$\alpha_{\text{LB}}(\boldsymbol{\mu}) \leq \alpha(\boldsymbol{\mu}) = \inf_{v \in X^{\mathcal{N}}} \frac{a(v, v; \boldsymbol{\mu})}{\|v\|_X^2}. \tag{32}$$

We also define the residual

$$r_N(v;\boldsymbol{\mu}) \equiv f(v;\boldsymbol{\mu}) - a(u_N(\boldsymbol{\mu}),v;\boldsymbol{\mu}) \tag{33}$$

for all $v \in X^{\mathcal{N}}$. In particular, with $e_N(\boldsymbol{\mu}) = u^{\mathcal{N}}(\boldsymbol{\mu}) - u_N(\boldsymbol{\mu})$, we have

$$a(e_N(\boldsymbol{\mu}),v;\boldsymbol{\mu}) = r_N(v;\boldsymbol{\mu}), \quad \forall v \in X^{\mathcal{N}}. \tag{34}$$

Hence, with $\hat{e}_N^{\mathcal{N}}(\boldsymbol{\mu}) \in X^{\mathcal{N}}$ that satisfies

$$a(\hat{e}_N^{\mathcal{N}}(\boldsymbol{\mu}),v;\bar{\boldsymbol{\mu}}) = r_N(v;\boldsymbol{\mu}), \quad \forall v \in X^{\mathcal{N}}, \tag{35}$$

we may write

$$\begin{aligned} a(e_N(\boldsymbol{\mu}),e_N(\boldsymbol{\mu});\boldsymbol{\mu}) &= a(\hat{e}_N^{\mathcal{N}}(\boldsymbol{\mu}),e_N(\boldsymbol{\mu});\bar{\boldsymbol{\mu}}) \\ &\le \|\hat{e}_N^{\mathcal{N}}(\boldsymbol{\mu})\|_X \|e_N(\boldsymbol{\mu})\|_X \\ &\le \|\hat{e}_N^{\mathcal{N}}(\boldsymbol{\mu})\|_X \frac{\|e_N(\boldsymbol{\mu})\|_{\boldsymbol{\mu}}}{(\alpha_{\mathrm{LB}}(\boldsymbol{\mu}))^{1/2}}, \end{aligned} \tag{36}$$

where we have used $v = e_N(\boldsymbol{\mu}) \in X^{\mathcal{N}}$ in (34) and (35), the Cauchy-Schwarz inequality and the definition (32) of the coercivity lower bound. Hence,

$$\|u^{\mathcal{N}}(\boldsymbol{\mu}) - u_N(\boldsymbol{\mu})\|_{\boldsymbol{\mu}} \le \frac{\|\hat{e}_N^{\mathcal{N}}(\boldsymbol{\mu})\|_X}{\big(\alpha_{\mathrm{LB}}(\boldsymbol{\mu})\big)^{1/2}} \equiv \Delta_N(\boldsymbol{\mu}), \tag{37}$$

where $\|\hat{e}_N^{\mathcal{N}}(\boldsymbol{\mu})\|_X = \sup_{v\in X^{\mathcal{N}}}(r_N(v;\boldsymbol{\mu})/\|v\|_X)$ is the dual norm of the residual. Again, due to the affinity assumptions (19), an efficient offline-online computational approach for $\Delta_N(\boldsymbol{\mu})$ can be developed. For a detailed derivation of (37) and the corresponding computational procedure, see [17, 19].

Now, we let $\tilde{X}^{\mathcal{N}} \supset X^{\mathcal{N}}$ be a discrete FE space identical to $X^{\mathcal{N}}$ except for the restriction on its members vanishing on Γ_0^{D}. Then we let $\psi^{\mathcal{N}}(\boldsymbol{\mu}) \in (V^\star \cap \tilde{X}^{\mathcal{N}})$ be the solution of the problem

$$a(v,\psi^{\mathcal{N}}(\boldsymbol{\mu});\boldsymbol{\mu}) = 0, \quad \forall v \in X^{\mathcal{N}}. \tag{38}$$

Note that since $\psi^{\mathcal{N}}(\boldsymbol{\mu}) \in (V^\star \cap \tilde{X}^{\mathcal{N}})$, we impose the essential Dirichlet condition $\psi^{\mathcal{N}}(\boldsymbol{\mu})|_{\Gamma_0^{\mathrm{D}}} = 1$.

Next, if we choose any $v^\star \in (V^\star \cap \tilde{X}^{\mathcal{N}})$, our "truth output" – to which the RB output will be compared – is given from (24) as

$$s^{\mathcal{N}}(\boldsymbol{\mu}) = a(u^{\mathcal{N}}(\boldsymbol{\mu}),v^\star;\boldsymbol{\mu}) - f(v^\star;\boldsymbol{\mu}), \tag{39}$$

and we obtain the error estimate

$$\begin{aligned} |s^{\mathcal{N}}(\boldsymbol{\mu}) - s_N(\boldsymbol{\mu};v^\star)| &= |a(u^{\mathcal{N}}(\boldsymbol{\mu}),v^\star;\boldsymbol{\mu}) - a(u_N(\boldsymbol{\mu}),v^\star;\boldsymbol{\mu})| \\ &= |a(e_N(\boldsymbol{\mu}),v^\star;\boldsymbol{\mu})| \\ &= |a(e_N(\boldsymbol{\mu}),v^\star - \psi^{\mathcal{N}}(\boldsymbol{\mu});\boldsymbol{\mu})| \\ &\le \|e_N(\boldsymbol{\mu})\|_{\boldsymbol{\mu}} \|v^\star - \psi^{\mathcal{N}}(\boldsymbol{\mu})\|_{\boldsymbol{\mu}}, \end{aligned} \tag{40}$$

by using the fact that $e_N(\boldsymbol{\mu}) \in X^{\mathcal{N}}$, that $\psi^{\mathcal{N}}(\boldsymbol{\mu})$ and $e_N(\boldsymbol{\mu})$ are orthogonal, and the Cauchy-Schwarz inequality. Thus, $|s^{\mathcal{N}}(\boldsymbol{\mu}) - s_N(\boldsymbol{\mu}; v^\star)| \leq \Delta_N(\boldsymbol{\mu})\|v^\star - \psi^{\mathcal{N}}(\boldsymbol{\mu})\|_{\boldsymbol{\mu}}$, and a good $v^\star$ is also a good approximation to $\psi^{\mathcal{N}}(\boldsymbol{\mu})$, making the term $\|v^\star - \psi^{\mathcal{N}}(\boldsymbol{\mu})\|_{\boldsymbol{\mu}}$ small.

To bound the term $\|v^\star - \psi^{\mathcal{N}}(\boldsymbol{\mu})\|_{\boldsymbol{\mu}}$, we view $v^\star$ as an approximation to $\psi^{\mathcal{N}}$, and define the residual $r_{v^\star}(v; \boldsymbol{\mu}) \equiv -a(v^\star, v; \boldsymbol{\mu})$. Analogously to (36), we have

$$\|v^\star - \psi^{\mathcal{N}}(\boldsymbol{\mu})\|_{\boldsymbol{\mu}} \leq \frac{\|\hat{e}^{\mathcal{N}}_{v^\star}(\boldsymbol{\mu})\|_X}{\big(\alpha_{\mathrm{LB}}(\boldsymbol{\mu})\big)^{1/2}} \equiv \Delta_{v^\star}(\boldsymbol{\mu}), \tag{41}$$

where $\hat{e}^{\mathcal{N}}_{v^\star}(\boldsymbol{\mu})$ belongs to $X^{\mathcal{N}}$ and solves $a(\hat{e}^{\mathcal{N}}_{v^\star}(\boldsymbol{\mu}), v; \bar{\boldsymbol{\mu}}) = r_{v^\star}(v; \boldsymbol{\mu})$ for all $v \in X^{\mathcal{N}}$. We thus arrive at

$$|s^{\mathcal{N}}(\boldsymbol{\mu}) - s_N(\boldsymbol{\mu}; v^\star)| \leq \Delta_N(\boldsymbol{\mu})\Delta_{v^\star}(\boldsymbol{\mu}) \equiv \Delta^{\mathrm{out}}_{N,v^\star}(\boldsymbol{\mu}) \tag{42}$$

as an upper bound for our output of interest.

Note that if we write $\psi^{\mathcal{N}}(\boldsymbol{\mu}) = \psi^{\mathcal{N},0}(\boldsymbol{\mu}) + \psi^{\mathrm{D}}$, where $\psi^{\mathrm{D}} \in (V^\star \cap \tilde{X}^{\mathcal{N}})$ is some chosen Dirichlet lift, we can write (38) as: Given $\boldsymbol{\mu} \in \mathcal{D}$, find $\psi^{\mathcal{N},0}(\boldsymbol{\mu}) \in X^{\mathcal{N}}$ such that

$$a(v, \psi^{\mathcal{N},0}(\boldsymbol{\mu}); \boldsymbol{\mu}) = -a(v, \psi^{\mathrm{D}}; \boldsymbol{\mu}), \quad \forall v \in X^{\mathcal{N}}. \tag{43}$$

Thus, if we choose ψ^{D} equal to $v^\star$, (43) is in fact the dual problem corresponding to the *primal* problem (23) with the output functional $l^{\mathrm{out}}(\cdot; \boldsymbol{\mu})$ given in (24), since $a(\cdot, v^\star; \boldsymbol{\mu})$ is the linear functional part of $l^{\mathrm{out}}(\cdot; \boldsymbol{\mu})$. We elaborate on this in Section 3.5.

3.4 "Good" flux lifting functions

We must keep two things in mind when choosing the flux lifting function $v^\star$. Firstly, it is important that the term $\|v^\star - \psi^{\mathcal{N}}(\boldsymbol{\mu})\|_{\boldsymbol{\mu}}$ in the estimate (40) is small. Secondly, we must make sure that the computational cost associated with the computation of $v^\star$ is small in the RB online stage.

Note that actually solving (38) for every new $\boldsymbol{\mu}$ and setting $v^\star = \psi^{\mathcal{N}}(\boldsymbol{\mu})$ will result in a zero error in the RB output, but obviously also in an unaffordable "truth FE complexity" online computational cost.

We next consider two alternative choices of "good" $v^\star$'s which both meet the two requirements mentioned above.

3.4.1 Coarse finite element approximation

Our first choice is to construct a coarse finite element approximation to $\psi^{\mathcal{N}}(\boldsymbol{\mu})$. That is to say, we first find $\psi^{\mathcal{M}}(\boldsymbol{\mu}) \in (V^\star \cap \tilde{X}^{\mathcal{M}}) \subset (V^\star \cap \tilde{X}^{\mathcal{N}})$ such that

$$a(v, \psi^{\mathcal{M}}(\boldsymbol{\mu}); \boldsymbol{\mu}) = 0, \quad \forall v \in X^{\mathcal{M}}, \tag{44}$$

where the coarse FE space $X^{\mathcal{M}} \subset X^{\mathcal{N}}$ has dimension $\mathcal{M} \ll \mathcal{N}$, and $\tilde{X}^{\mathcal{M}}$ is equal to $X^{\mathcal{M}}$ except for the restriction on its members vanishing on Γ^{D}_0. We

then choose $v^\star = \psi^{\mathcal{M}}(\boldsymbol{\mu})$ as the flux lifting function. In particular, $\mathcal{M}$ should here be chosen small enough that it is affordable to compute $\psi^{\mathcal{M}}(\boldsymbol{\mu})$ in the RB online stage, without compromising the rapid online RB output evaluation.

Now, to bound the term $\|\psi^{\mathcal{M}}(\boldsymbol{\mu}) - \psi^{\mathcal{N}}(\boldsymbol{\mu})\|_{\boldsymbol{\mu}}$, we use the result (41) to arrive at $\|\psi^{\mathcal{M}}(\boldsymbol{\mu}) - \psi^{\mathcal{N}}(\boldsymbol{\mu})\|_{\boldsymbol{\mu}} \leq \Delta_{\mathcal{M}}(\boldsymbol{\mu})$ (we here use $_{\mathcal{M}}$ to indicate that the $v^\star$ in (41) is now a coarse FE approximation to $\psi^{\mathcal{N}}(\boldsymbol{\mu})$). Then, we define $\Delta^{\text{out}}_{N,\mathcal{M}}(\boldsymbol{\mu}) \equiv \Delta_N(\boldsymbol{\mu})\Delta_{\mathcal{M}}(\boldsymbol{\mu})$, and conclude that for all $\boldsymbol{\mu} \in \mathcal{D}$,

$$\left|s^{\mathcal{N}}(\boldsymbol{\mu}) - s_N(\boldsymbol{\mu}; \psi^{\mathcal{M}}(\boldsymbol{\mu}))\right| \leq \Delta^{\text{out}}_{N,\mathcal{M}}(\boldsymbol{\mu}). \tag{45}$$

3.4.2 Reference parameter approximation

Alternatively, we may take $v^\star = \psi^{\mathcal{N}}(\bar{\boldsymbol{\mu}})$ as our approximation of $\psi^{\mathcal{N}}(\boldsymbol{\mu})$ for any $\boldsymbol{\mu} \in \mathcal{D}$. Since $v^\star = \psi^{\mathcal{N}}(\bar{\boldsymbol{\mu}})$ is the solution to (38) for the preselected reference parameter, it can be precomputed in the RB offline stage and then reused every time we evaluate the RB output of interest, without any additional RB online cost.

From (41), an upper bound for the term $\|\psi^{\mathcal{N}}(\boldsymbol{\mu}) - \psi^{\mathcal{N}}(\bar{\boldsymbol{\mu}})\|_{\boldsymbol{\mu}}$ is given by $\Delta_{\bar{\boldsymbol{\mu}}}(\boldsymbol{\mu})$ (where we substitute $_{\bar{\boldsymbol{\mu}}}$ for $_{v^\star}$ to remember our particular choice for $v^\star$). We thus get

$$|s^{\mathcal{N}}(\boldsymbol{\mu}) - s_N(\boldsymbol{\mu}; \psi^{\mathcal{N}}(\bar{\boldsymbol{\mu}}))| \leq \Delta_N(\boldsymbol{\mu})\Delta_{\bar{\boldsymbol{\mu}}}(\boldsymbol{\mu}) \equiv \Delta^{\text{out}}_{N,\bar{\boldsymbol{\mu}}}(\boldsymbol{\mu}) \tag{46}$$

as an upper bound for the error in the RB output of interest.

3.5 Primal-dual RB approximation

Evidently, one way to approximate $\psi^{\mathcal{N}}(\boldsymbol{\mu})$ is by way of a reduced basis approximation $\psi_M(\boldsymbol{\mu})$. The RB problem corresponding to (43) (and (38)) reads: Find $\psi^0_M(\boldsymbol{\mu}) \in X^{\text{du}}_M$ such that

$$a(v, \psi^0_M(\boldsymbol{\mu}); \boldsymbol{\mu}) = -a(v, \psi^{\text{D}}; \boldsymbol{\mu}), \quad \forall v \in X^{\text{du}}_M, \tag{47}$$

and set $\psi_M(\boldsymbol{\mu}) = \psi^0_M(\boldsymbol{\mu}) + \psi^{\text{D}}$. Here, X^{du}_M denotes the RB dual approximation space, given by

$$X^{\text{du}}_M = \text{span}\{\psi^{\mathcal{N}}(\boldsymbol{\mu}_m) - \psi^{\text{D}}\}_{m=1}^M, \tag{48}$$

where the $\psi^{\mathcal{N}}(\boldsymbol{\mu}_m)$ are snapshots taken of $\psi^{\mathcal{N}}$ at M different points in parameter space. In fact, the formulation of the two problems (26) and (47), together with the output of interest given in (27), corresponds to a standard RB primal-dual formulation [17, 19], which is the standard way of speeding up the convergence of RB solutions to general non-compliant problems. Let us spend a few lines elaborating on this.

First, we choose a $v^\star \in (V^\star \cap \tilde{X}^{\mathcal{N}})$ and let $\psi^{\text{D}} = v^\star$. Hence, the right-hand-side of (47) is precisely the linear functional part of the output functional (with

a minus sign), and $v^\star$ is the Dirichlet lifting function for the dual problem. The standard "dual-corrected" RB output reads

$$\hat{s}_{M,N}(\boldsymbol{\mu}) \equiv s_N(\boldsymbol{\mu}; \psi^{\mathrm{D}}) - r_N(\psi_M^0(\boldsymbol{\mu}); \boldsymbol{\mu}), \tag{49}$$

where $r_N(v; \boldsymbol{\mu}) = f(v; \boldsymbol{\mu}) - a(u_N(\boldsymbol{\mu}), v; \boldsymbol{\mu})\big)$ is the primal residual and $\psi_M^0(\boldsymbol{\mu})$ is the homogeneous part of the solution to (47). In the below expression, we drop the argument $\boldsymbol{\mu}$ of functions in all intermediate steps for brevity. With $e_N(\boldsymbol{\mu}) = u^{\mathcal{N}}(\boldsymbol{\mu}) - u_N(\boldsymbol{\mu})$, we see that

$$\begin{aligned}
|s^{\mathcal{N}}(\boldsymbol{\mu}) - \hat{s}_{M,N}(\boldsymbol{\mu})| &= |s^{\mathcal{N}}(\boldsymbol{\mu}) - s_N(\boldsymbol{\mu}; \psi^{\mathrm{D}}) + r_N(\psi_M^0; \boldsymbol{\mu})| \\
&= |a(e_N, \psi^{\mathrm{D}}; \boldsymbol{\mu}) + r_N(\psi_M^0; \boldsymbol{\mu})| \\
&= |a(e_N, \psi^{\mathcal{N},0}; \boldsymbol{\mu}) - r_N(\psi_M^0; \boldsymbol{\mu})| \\
&= |a(e_N, \psi^{\mathcal{N},0}; \boldsymbol{\mu}) - a(u_N, \psi_M^0; \boldsymbol{\mu}) + f(\psi_M^0; \boldsymbol{\mu})| \\
&= |a(e_N, \psi^{\mathcal{N},0}; \boldsymbol{\mu}) - a(u_N, \psi_M^0; \boldsymbol{\mu}) + a(u^{\mathcal{N}}, \psi_M^0; \boldsymbol{\mu})| \\
&= |a(e_N, \psi^{\mathcal{N},0} - \psi_M^0; \boldsymbol{\mu})| \\
&\leq \|e_N\|_{\boldsymbol{\mu}}(\boldsymbol{\mu}) \|\psi^{\mathcal{N},0}(\boldsymbol{\mu}) - \psi_M^0(\boldsymbol{\mu})\|_{\boldsymbol{\mu}}.
\end{aligned} \tag{50}$$

In the two first steps, we here use the expression (49) for $\hat{s}_{M,N}$ and then arbitrarity (up to functions in $(V^\star \cap \tilde{X}^{\mathcal{N}})$) of the flux lifting function for the "truth" output (we can thus write $s^{\mathcal{N}}(\boldsymbol{\mu}) - s_N(\boldsymbol{\mu}; \psi^{\mathrm{D}}) = a(e_N(\boldsymbol{\mu}), \psi^{\mathrm{D}}; \boldsymbol{\mu})$). In the third and fourth steps, we invoke (43) with $v = -e_N(\boldsymbol{\mu})$ and then (33) with $v = \psi_M^0$. Next, we use the definition of the "truth" primal problem, then linearity and lastly the Cauchy-Schwarz inequality. Hence, if we solve the RB primal and dual problems in parallel with $M \approx N$, we get a "quadratic" effect in the convergence of the output of interest.

Next, it is straightforward to deduce that $\hat{s}_{M,N}(\boldsymbol{\mu}) = s_N(\boldsymbol{\mu}; \psi_M(\boldsymbol{\mu}))$, i.e., that these two output evaluations are equivalent. We start with the expression (49), and then appeal to the (bi)linearity of $a(\cdot, \cdot; \boldsymbol{\mu})$ and $f(\cdot; \boldsymbol{\mu})$. Again, we drop the $\boldsymbol{\mu}$-dependence of functions for typesetting convenience:

$$\begin{aligned}
\hat{s}_{M,N}(\boldsymbol{\mu}) &= s_N(\boldsymbol{\mu}; \psi^{\mathrm{D}}) - r_N(\psi_M^0; \boldsymbol{\mu}) \\
&= a(u_N, \psi^{\mathrm{D}}; \boldsymbol{\mu}) + a(u_N, \psi_M^0; \boldsymbol{\mu}) - f(\psi^{\mathrm{D}}; \boldsymbol{\mu}) - f(\psi_M^0; \boldsymbol{\mu}) \\
&= a(u_N, \psi^{\mathrm{D}} + \psi_M^0; \boldsymbol{\mu}) - f(\psi^{\mathrm{D}} + \psi_M^0; \boldsymbol{\mu}) \\
&= s_N(\boldsymbol{\mu}; \psi_M).
\end{aligned} \tag{51}$$

In other words, the standard dual-corrected output with $v^\star = \psi^{\mathrm{D}}$ produces the same result as the non-corrected output with $v^\star = \psi_M(\boldsymbol{\mu}) = \psi_M^0(\boldsymbol{\mu}) + \psi^{\mathrm{D}}$. Thus, for flux integral outputs, the standard RB primal-dual approximation framework may be viewed as a technique for improving upon any initial choice made for $v^\star$.

Up to this point, we have only considered a single output of interest. Surely, it could in a practical application be desirable to evaluate several outputs of interest, all being functionals of the solution of the same underlying PDE. For

example, we might want the integral of the flux through J entire disjoint sections $\Gamma_0^{\mathrm{D}}, \Gamma_1^{\mathrm{D}}, \ldots, \Gamma_{J-1}^{\mathrm{D}}$ of the boundary, resulting in J different output functionals and thus in turn J different dual problems. Of course, in the case of multiple outputs, no more than one can be compliant.

When J is small, solving the primal and dual problems in parallel with (say) $M \approx N$ basis functions may drastically reduce the RB output error(s) and error bound(s). However, for many outputs (large J), online computation of the solution to every corresponding dual problem (when $M \approx N$) may be impracticable – $\mathcal{O}(N^3)$ and $\mathcal{O}(M^3)$ operations are required for direct computation of the solutions to the primal and dual RB problems, respectively – and we are thus forced to trade numerical accuracy for computational speed. In this situation, choosing good flux lifting functions seems important.

On the other hand, if we do proceed with RB approximations to the solution(s) to the dual problem(s) as well, making good choices for the dual Dirichlet liftings would surely be of interest (obviously, $\psi^{\mathrm{D}} = \psi^{\mathcal{N}}(\boldsymbol{\mu})$ would be the optimal, though an impractical, choice).

3.6 Computational approach for output evaluation

In the RB online stage, and without regard to our particular choice for $v^\star$, we need to compute

$$s_N(\boldsymbol{\mu}) = l^{\mathrm{out}}(u_N(\boldsymbol{\mu})) = a(u_N(\boldsymbol{\mu}), v^\star; \boldsymbol{\mu}) - f(v^\star; \boldsymbol{\mu}), \tag{52}$$

once the RB solution is obtained. Note that also when we pursue a primal-dual approximation, we are still left with an evaluation on this form, due to the result (51).

Since, for each $\boldsymbol{\mu} \in \mathcal{D}$, $a(\cdot, \cdot; \boldsymbol{\mu})$ and $f(\cdot; \boldsymbol{\mu})$ are, by assumption, parametrically affine, $l^{\mathrm{out}}(\cdot; \boldsymbol{\mu})$ will also be parametrically affine. Hence, we can compute the RB output at an additional computational cost of $\mathcal{O}(N)$ operations. To see this, we write $a(v, w; \boldsymbol{\mu})$ and $f(v; \boldsymbol{\mu})$ in their parametrically affine expansions (19) as

$$a(v, w; \boldsymbol{\mu}) = \sum_{q=1}^{Q_a} a^q(v, w)\Theta_a^q(\boldsymbol{\mu}), \qquad f(v; \boldsymbol{\mu}) = \sum_{q=1}^{Q_f} f^q(v)\Theta_f^q(\boldsymbol{\mu}), \tag{53}$$

for any $v, w \in X$. With $u_N(\boldsymbol{\mu}) = \sum_{n=1}^N u_{N,n}(\boldsymbol{\mu})\zeta_n$, where the ζ_n are the orthogonalised RB basis functions (in order to get a reduced system of equations that is well conditioned, the basis functions $u^{\mathcal{N}}(\boldsymbol{\mu}_n)$, $1 \le n \le N$, are orthogonalised with respect to the norm $\|\cdot\|_X$, cf. [19]) and $u_{N,n}(\boldsymbol{\mu})$ are the RB solution

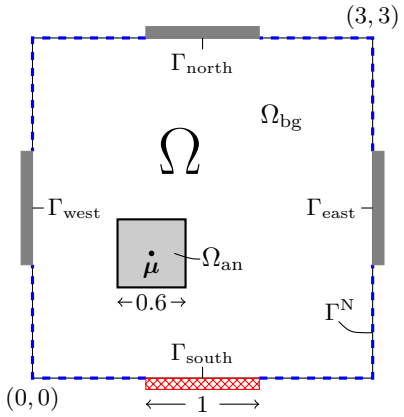

Figure 3: Physical domain Ω with an electrode attached to each edge.

coefficients, we get

$$l^{\text{out}}(u_N(\boldsymbol{\mu})) = \sum_{q=1}^{Q_a} a^q(u_N(\boldsymbol{\mu}), v^\star)\Theta_a^q(\boldsymbol{\mu}) - \sum_{q=1}^{Q_f} f^q(v^\star)\Theta_f^q(\boldsymbol{\mu})$$
$$= \sum_{n=1}^{N} u_{N,n}(\boldsymbol{\mu}) \sum_{q=1}^{Q_a} a^q(\zeta_n, v^\star)\Theta_a^q(\boldsymbol{\mu}) - \sum_{q=1}^{Q_f} f^q(v^\star)\Theta_f^q(\boldsymbol{\mu}), \qquad (54)$$

which is a $Q_a N + Q_f$ operations summation, assuming that the values $a^q(\zeta_n, v^\star)$, $1 \le q \le Q_a$, and $f^q(v^\star)$, $1 \le q \le Q_f$ are precomputed in the RB offline stage, and that the function values $\Theta_a^q(\boldsymbol{\mu})$ and $\Theta_f^q(\boldsymbol{\mu})$ are readily computable. Note that we have here assumed for simplicity that $v^\star$ is $\boldsymbol{\mu}$-independent (according to, for example, the reference parameter approximation discussed in Section 3.4.2).

Thus far, we have assumed that a and f are parametrically affine. In the more general case of a non-affine problem, it is possible to construct parametrically affine expansions that are good *approximations* of $a(\cdot, \cdot; \boldsymbol{\mu})$ and $f(\cdot; \boldsymbol{\mu})$ for any $\boldsymbol{\mu} \in \mathcal{D}$ by invoking the *empirical interpolation* method [3, 9, 14]. In this case, the additional computational cost for output evaluation is still only $\mathcal{O}(N)$ in the RB online stage, but the RB problem solved is slightly modified.

4 An Illustrative Example

4.1 Problem formulation

We consider the electrostatic potential, u, inside a square domain $\Omega = (0, 3) \times (0, 3)$ which contains an "insulating" square anomaly, Ω_{an}, with edges of length 0.6, as depicted in Figure 3.

Attached to the boundary of Ω, $\partial\Omega$, are four electrodes of unity length, centred on each of the edges of Ω. The electrodes constitute the Dirichlet

boundary $\Gamma^{\mathrm{D}} \equiv \Gamma_{\mathrm{south}} \cup \Gamma_{\mathrm{north}} \cup \Gamma_{\mathrm{east}} \cup \Gamma_{\mathrm{west}}$, on which the potential is presicribed as

$$u = \begin{cases} 1, & \text{on } \Gamma_{\mathrm{south}}, \\ 0, & \text{on } \Gamma_{\mathrm{north}} \cup \Gamma_{\mathrm{east}} \cup \Gamma_{\mathrm{west}}. \end{cases} \tag{55}$$

On the Neumann boundary, $\Gamma^{\mathrm{N}} \equiv \partial\Omega \setminus \Gamma^{\mathrm{D}}$, we assume electrostatic insulation, i.e.

$$\frac{\partial u}{\partial n} = 0, \quad \text{on } \Gamma^{\mathrm{N}}. \tag{56}$$

We define the "background material" as $\Omega_{\mathrm{bg}} \equiv \Omega \setminus \overline{\Omega}_{\mathrm{an}}$. The electric permittivity, ϵ, inside Ω is given as

$$\epsilon \equiv \begin{cases} \epsilon_{\mathrm{bg}} \equiv 1, & \text{in } \Omega_{\mathrm{bg}}, \\ \epsilon_{\mathrm{an}} \equiv 0.1, & \text{in } \Omega_{\mathrm{an}}. \end{cases} \tag{57}$$

Finally, in $\Omega_{\mathrm{bg}} \cup \Omega_{\mathrm{an}}$, the electrostatic potential is governed by the Laplace equation,

$$-\nabla^2 u = 0. \tag{58}$$

Our problem is parameterised by the parameter vector $\boldsymbol{\mu} \equiv (\mu_1, \mu_2) \in \mathcal{D}$, which determines the position of the centre of Ω_{an}. Here, $\mathcal{D} \subset \Omega$ is our parameter domain, defined as $\mathcal{D} \equiv [1,2] \times [1,2]$. Hence, the shape of Ω_{bg} and the position of Ω_{an} depend upon $\boldsymbol{\mu}$. For typesetting convenience however, we do not explicitly denote these dependencies in formulas.

Our output of interest is the accumulated charge on the eastern electrode, i.e., the capacitance corresponding to the "south-east" pair of electrodes, given by the flux integral

$$\tilde{s}(\boldsymbol{\mu}) \equiv -\epsilon_{\mathrm{bg}} \int_{\Gamma_{\mathrm{east}}} \frac{\partial u(\boldsymbol{\mu})}{\partial n} \, \mathrm{d}s. \tag{59}$$

4.2 RB treatment

4.2.1 Parameterised weak form

Let $u^{\mathrm{D}} \in H^1$ be a lifting of the Dirichlet data (55), and write $u(\boldsymbol{\mu}) = u^0(\boldsymbol{\mu}) + u^{\mathrm{D}}$. With the boundary conditions (55) and (56), together with the assumption of flux continuity on the interior boundary and global continuity of the solution, the parametric weak form of our problem reads: Given any $\boldsymbol{\mu} \in \mathcal{D}$, find $u^0(\boldsymbol{\mu}) \in X$ such that

$$a(u(\boldsymbol{\mu}), v; \boldsymbol{\mu}) = 0, \quad \forall v \in X, \tag{60}$$

where $u(\boldsymbol{\mu}) = u^0(\boldsymbol{\mu}) + u^{\mathrm{D}}$,

$$a(u, v; \boldsymbol{\mu}) = \epsilon_{\mathrm{bg}} \int_{\Omega_{\mathrm{bg}}} \nabla u \cdot \nabla v \, \mathrm{d}\Omega + \epsilon_{\mathrm{an}} \int_{\Omega_{\mathrm{an}}} \nabla u \cdot \nabla v \, \mathrm{d}\Omega \tag{61}$$

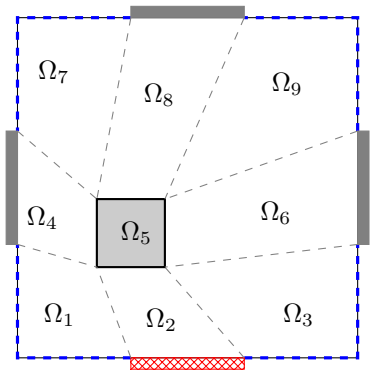

Figure 4: Decomposition of the physical domain into nine (deformed square) spectral elements.

and $X = \{v \in H^1 : v|_{\Gamma^{\mathrm{D}}} = 0\}$.

In order to treat our problem numerically, we decompose our domain into nine subdomains, as depicted in Figure 4. Next, we introduce a reference domain $\hat{\Omega} \equiv (-1,1) \times (-1,1)$ and standard transfinite mappings [8] $\mathcal{F}_i : \Omega_i \to \hat{\Omega}$, $1 \leq i \leq 9$. We may then write our bilinear form, a, in terms of the reference variables (ξ, η) on the reference domain $\hat{\Omega} \equiv (-1,1) \times (-1,1)$ via the mappings $\mathcal{F}_i$ as

$$a(u, v; \boldsymbol{\mu}) = \sum_{i=1}^{9} \epsilon_i \int_{\hat{\Omega}} (\hat{\nabla} \hat{u}_i)^{\mathrm{T}} G_i(\boldsymbol{\mu}) \hat{\nabla} \hat{v}_i \, \mathrm{d}\hat{\Omega}, \tag{62}$$

where $\hat{\nabla}$ is the gradient operator in the reference variables and, for $1 \leq i \leq 9$, ϵ_i denotes the electric permittivity in Ω_i, $\hat{v}_i(\xi, \eta) \equiv v(x, y)|_{\Omega_i} \circ \mathcal{F}_i$, and G_i is a parametrically and spatially dependent 2×2 symmetric positive definite matrix comprising the geometrical factors induced by $\mathcal{F}_i$.

4.2.2 "Truth" spectral element approximation

In order to construct the snapshots upon which to build the RB approximations, we define the "truth" discretisation of (60). To this end, we shall employ a standard spectral element method based on high-order polynomials [15].

As our discrete "truth" approximation space, we define

$$X^{\mathcal{N}} \equiv \{v \in H^1(\Omega) : v|_{\Gamma^{\mathrm{D}}} = 0, \hat{v}_i \in \mathbb{P}_P(\hat{\Omega}), 1 \leq i \leq 9\}, \tag{63}$$

where $\mathbb{P}_P(\hat{\Omega})$ denotes the space of polynomials of degree P in each direction over $\hat{\Omega}$. With $\mathcal{N} = \dim(X^{\mathcal{N}})$, we note that $\mathcal{N} \sim P^2$. For the Dirichlet and flux lifting functions, we shall also use (mapped) polynomials. We thus require the

spaces

$$\tilde{X}^{\mathcal{N}}_{\text{east}} \equiv \{v \in H^1(\Omega) : v|_{\Gamma^{\text{D}}\setminus\Gamma_{\text{east}}} = 0, \hat{v}_i \in \mathbb{P}_P(\hat{\Omega}), 1 \le i \le 9\}, \tag{64}$$

$$\tilde{X}^{\mathcal{N}}_{\text{south}} \equiv \{v \in H^1(\Omega) : v|_{\Gamma^{\text{D}}\setminus\Gamma_{\text{south}}} = 0, \hat{v}_i \in \mathbb{P}_P(\hat{\Omega}), 1 \le i \le 9\}, \tag{65}$$

and we also define

$$V^\star \equiv \{v \in H^1 : v|_{\Gamma^{\text{D}}\setminus\Gamma_{\text{east}}} = 0, v|_{\Gamma_{\text{east}}} = 1\}. \tag{66}$$

We now state the "truth" discretisation of (60) as: For any $\boldsymbol{\mu} \in \mathcal{D}$, find $u^{\mathcal{N},0}(\boldsymbol{\mu}) \in X^{\mathcal{N}}$ such that

$$a(u^{\mathcal{N}}(\boldsymbol{\mu}), v; \boldsymbol{\mu}) = 0, \quad \forall v \in X^{\mathcal{N}}, \tag{67}$$

where $u^{\mathcal{N}}(\boldsymbol{\mu}) = u^{\mathcal{N},0}(\boldsymbol{\mu}) + u^{\text{D}}$ and $u^{\text{D}} \in \tilde{X}^{\mathcal{N}}_{\text{east}}$ is some chosen ($\boldsymbol{\mu}$-independent) lifting of the Dirichlet data (55). The corresponding "truth" output of interest is

$$s^{\mathcal{N}}(\boldsymbol{\mu}) = l^{\text{out}}(u^{\mathcal{N}}(\boldsymbol{\mu})) = a(u^{\mathcal{N}}(\boldsymbol{\mu}), v^\star; \boldsymbol{\mu}), \tag{68}$$

In (68), we have omitted the minus sign (that appeared in (59) since the capacitance is positive by definition). Also note that for the "truth" problem, any two $v^\star \in (V^\star \cap \tilde{X}^{\mathcal{N}}_{\text{south}})$ will produce the same numerical output, as we saw in Section 2.

As basis functions for the three discrete spaces above, and as shape functions for the "truth" approximations, we use the Lagrange polynomials over the $(P+1)^2$ tensorised GLL nodes (on $\hat{\Omega}$) [5]. Specifically, we have made the choice $P = 35$.

Due to the change from Neumann to Dirichlet boundary conditions at the electrode edges, u exhibits known singularities [2, 11] which will limit the convergence of the high order polynomial approximation. Although there exist techniques to improve the finite element convergence rate when singularities are present, (e.g. using an adaptive h-p finite element method [2]) we restrict ourselves here to a standard spectral element approximation based on high order polynomials since our focus in this paper is the accuracy of the RB approximation relative to the "truth" approximation.

4.2.3 Reduced basis approximation

The RB approximation spaces are defined as

$$X_N \equiv \text{span}\{u_0^{\mathcal{N}}(\boldsymbol{\mu}_n)\}_{n=1}^N, \tag{69}$$

for $1 \le N \le N_{\max}$. If we move the term comprising the Dirichlet lifting to the right-hand-side, the RB problem may be written as: For any $\boldsymbol{\mu} \in \mathcal{D}$, find $u_N^0(\boldsymbol{\mu}) \in X_N$ such that

$$a(u_N^0(\boldsymbol{\mu}), v; \boldsymbol{\mu}) = -a(u^{\text{D}}, v; \boldsymbol{\mu}), \quad \forall v \in X_N, \tag{70}$$

and set $u_N(\boldsymbol{\mu}) = u_N^0(\boldsymbol{\mu}) + u^{\mathrm{D}}$. We then evaluate our output of interest as

$$s_N(\boldsymbol{\mu}; v^\star) \equiv a(u_N(\boldsymbol{\mu}), v^\star; \boldsymbol{\mu}), \tag{71}$$

where we choose $v^\star \in (V^\star \cap \tilde{X}^{\mathcal{N}}_{\mathrm{south}})$.

In order to construct X_N, $1 \leq N \leq N_{\max}$, we use the greedy parameter selection process outlined in Section 3.1.3. We start by choosing $\boldsymbol{\mu}_1$ randomly from $\mathcal{D}$ and then compute the corresponding first snapshot $u^{\mathcal{N},0}(\boldsymbol{\mu}_1)$. Next, for $2 \leq N \leq N_{\max}$, we choose $\boldsymbol{\mu}_N$ from a training sample $\Xi_{\mathrm{train}} \subset \mathcal{D}$ in a greedy manner based on *a posteriori* upper bounds $\Delta_{N-1}(\boldsymbol{\mu})$ – computed for every $\boldsymbol{\mu} \in \Xi_{\mathrm{train}}$ – for the energy-norm errors $\|u^{\mathcal{N},0}(\boldsymbol{\mu}) - u^0_{N-1}(\boldsymbol{\mu})\|_{\boldsymbol{\mu}}$, and then compute the next snapshot as $u^{\mathcal{N},0}(\boldsymbol{\mu}_N)$. (A detailed description of the procedure can be found in [19].) Here, we have chosen Ξ_{train} as an equidistant "grid" of 225 points in $\mathcal{D}$.

Unfortunately, the elements of the matrices G_k do not permit a parametrically affine expansion of a, as assumed in (19). For this reason, our computations do not immediately decouple to the very desirable offline and online stages. However, as commented in the previous section, the empirical interpolation method provides means to this end [3, 9, 14]. In fact, we can make the empirical interpolation error negligible if we make sure to include enough terms in the approximate affine expansion of a. If the number of required terms is not too large, we can at the same time use an efficient offline-online computational approach. In the numerical tests that follow, however, we have chosen to not use an offline-online decoupling approach, since this is not critical for our conclusions.

4.2.4 *A posteriori* error estimation: a coercivity lower bound

If we were to use an offline-online decoupling approach for our particular problem, we should also include additional terms in the *a posteriori* error estimators in order to account for the empirical interpolation error [3, 16]. However, the standard estimators from Section 3 are still valid under the assumption of a negligible interpolation error because the additional terms will vanish as the interpolation error goes to zero. Hence, if we for any $\boldsymbol{\mu} \in \mathcal{D}$ can establish a coercivity lower bound $\alpha_{\mathrm{LB}}(\boldsymbol{\mu})$, we can compute an energy-norm error bound $\Delta_N(\boldsymbol{\mu})$ and output error bounds $\Delta^{\mathrm{out}}_{N,\mathcal{M}}(\boldsymbol{\mu})$ and $\Delta^{\mathrm{out}}_{N,\bar{\boldsymbol{\mu}}}(\boldsymbol{\mu})$ as described in Sections 3.3, 3.4.1 and 3.4.2. In fact, if we for $1 \leq k \leq 9$ let $\sigma_k(\boldsymbol{\mu})$ denote the set of eigenvalues of the (symmetric and positive definite) matrix $G_k(\boldsymbol{\mu})$ of geometrical factors, and define

$$\lambda^-(\boldsymbol{\mu}) \equiv \min_{\substack{(\xi,\eta)\in\hat{\Omega} \\ 1\leq k\leq 9}} \sigma_k(\xi, \eta; \boldsymbol{\mu}), \quad \lambda^+(\boldsymbol{\mu}) \equiv \max_{\substack{(\xi,\eta)\in\hat{\Omega} \\ 1\leq k\leq 9}} \sigma_k(\xi, \eta; \boldsymbol{\mu}), \tag{72}$$

it can be shown (c.f. [7, 13]) that a coercivity lower bound for our particular problem is given by

$$\alpha_{\mathrm{LB}}(\boldsymbol{\mu}) = \frac{\lambda^-(\boldsymbol{\mu})}{\lambda^+(\bar{\boldsymbol{\mu}})}. \tag{73}$$

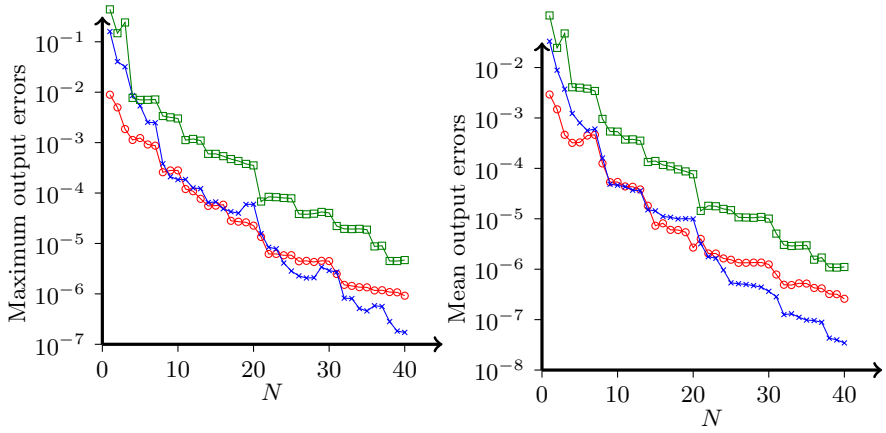

Figure 5: Maximum (left) and mean (right) of the output errors $e_N^{\text{out}}(\boldsymbol{\mu}; v^\star)$ over Ξ_{test} for the three choices $\psi^{\mathcal{N}}(\bar{\boldsymbol{\mu}})$ ($\times$), $\psi^{\mathcal{M}_2}(\boldsymbol{\mu})$ ($\circ$) and $v^\star_{\text{naive}}$ ($\square$) for $v^\star$, as functions of the number of reduced basis functions, N.

Our particular choice for the reference parameter vector is $\bar{\boldsymbol{\mu}} = (1.5, 1.5)$, i.e., the centre of $\mathcal{D}$. We make a remark here that the maximum and minimum of the $\sigma_k(\cdot, \cdot; \boldsymbol{\mu})$ are in practice realised over the tensorised GLL nodes.

4.3 Numerical results

Here, we present results for the RB output error, defined as

$$e_N^{\text{out}}(\boldsymbol{\mu}; v^\star) \equiv |s_N(\boldsymbol{\mu}; v^\star) - s^{\mathcal{N}}(\boldsymbol{\mu})|, \tag{74}$$

and the RB output error bound $\Delta_{N,v^\star}^{\text{out}}(\boldsymbol{\mu})$. For $v^\star \in (V^\star \cap \tilde{X}^{\mathcal{N}}_{\text{south}})$, we shall make use of three different functions: The reference parameter approximation $\psi^{\mathcal{N}}(\bar{\boldsymbol{\mu}})$ discussed in Section 3.4.2 with $\bar{\boldsymbol{\mu}} = (1.5, 1.5)$, the coarse finite element approximation $\psi^{\mathcal{M}_2}(\boldsymbol{\mu})$ discussed in Section 3.4.1, which corresponds to the solution of (44) using quadratic polynomials as basis functions, and a "naive" choice, $v^\star_{\text{naive}}$, given as

$$v^\star_{\text{naive}} \equiv \begin{cases} 1, & \text{on } \Gamma_{\text{east}}, \\ 0, & \text{at every other GLL node.} \end{cases} \tag{75}$$

Note that in a spectral element context, the naive choice would be the natural and computationally convenient choice to make for $v^\star$.

In order to test the RB approximations, we introduce a test sample $\Xi_{\text{test}} \subset \mathcal{D}$ consisting of 200 random points with a uniform distribution over $\mathcal{D}$. We assume that Ξ_{test} is dense enough that the behavior of the RB output for $\boldsymbol{\mu} \in \Xi_{\text{test}}$ gives a good representation of the behavior of the RB output for all $\boldsymbol{\mu} \in \mathcal{D}$.

In Figure 5, we plot the maximum (to the left) and mean (to the right) of the output errors $e_N^{\text{out}}(\boldsymbol{\mu}; \psi^{\mathcal{N}}(\bar{\boldsymbol{\mu}}))$, $e_N^{\text{out}}(\boldsymbol{\mu}; \psi^{\mathcal{M}_2}(\boldsymbol{\mu}))$ and $e_N^{\text{out}}(\boldsymbol{\mu}; v^\star_{\text{naive}})$ over all $\boldsymbol{\mu} \in$

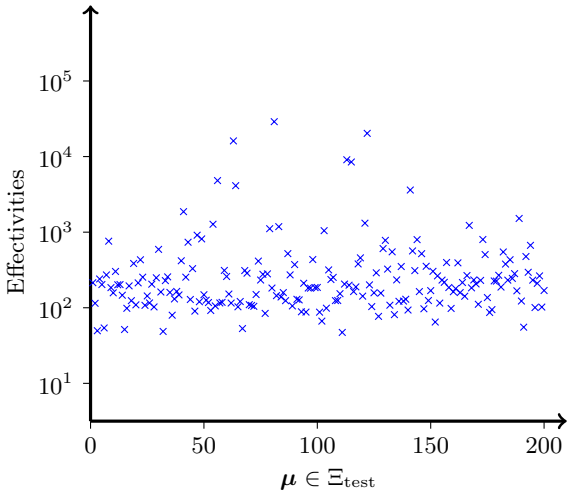

Figure 6: Output error bound effectivity $\nu^{\text{out}}_{N,\bar{\boldsymbol{\mu}}}(\boldsymbol{\mu})$ for all $\boldsymbol{\mu} \in \Xi_{\text{test}}$ for $N = 25$ (in no particular order).

Ξ_{test} as a function of the number of RB basis functions, N. We conclude that the two "good" choices for $v^\star$ in general perform about an order of magnitude better than the naive choice.

Next, for all $\boldsymbol{\mu} \in \Xi_{\text{test}}$, and for the particular case of $N = 25$, we compute the *effectivity* associated with the output error estimator $\Delta^{\text{out}}_{N,\bar{\boldsymbol{\mu}}}$, defined as

$$\nu^{\text{out}}_{N,\bar{\boldsymbol{\mu}}}(\boldsymbol{\mu}) \equiv \frac{\Delta^{\text{out}}_{N,\bar{\boldsymbol{\mu}}}(\boldsymbol{\mu})}{e^{\text{out}}_N(\boldsymbol{\mu}; \psi^{\mathcal{N}}(\bar{\boldsymbol{\mu}}))}. \tag{76}$$

Associated with the other two choices for $v^\star$, we define the effectivities $\nu^{\text{out}}_{N,\mathcal{M}_2}(\boldsymbol{\mu})$ and $\nu^{\text{out}}_{N,v^\star_{\text{naive}}}(\boldsymbol{\mu})$ in a similar way. For most $\boldsymbol{\mu} \in \Xi_{\text{test}}$, the effectivity $\nu^{\text{out}}_{N,\bar{\boldsymbol{\mu}}}(\boldsymbol{\mu})$ is in the range $\mathcal{O}(100) < \nu^{\text{out}}_{N,\bar{\boldsymbol{\mu}}}(\boldsymbol{\mu}) < \mathcal{O}(1000)$, as shown in Figure 6. For the other two effectivities, $\nu^{\text{out}}_{N,\mathcal{M}_2}(\boldsymbol{\mu})$ and $\nu^{\text{out}}_{N,v^\star_{\text{naive}}}(\boldsymbol{\mu})$, the results are similar (not shown). We also find that, for most $\boldsymbol{\mu} \in \Xi_{\text{test}}$, $\nu^{\text{out}}_{N,\mathcal{M}_2}(\boldsymbol{\mu}) < \nu^{\text{out}}_{N,\bar{\boldsymbol{\mu}}}(\boldsymbol{\mu}) < \nu^{\text{out}}_{N,v^\star_{\text{naive}}}(\boldsymbol{\mu})$. This is, however, not generally true for other choices of N.

The reason for the output error estimators being rather conservative is the large "angle" between the error of the primal problem, $u_N(\boldsymbol{\mu}) - u^{\mathcal{N}}(\boldsymbol{\mu})$, and the error of the dual problem, $\psi^{\mathcal{N}}(\bar{\boldsymbol{\mu}}) - \psi^{\mathcal{N}}(\boldsymbol{\mu})$. Thus, the Cauchy-Schwarz inequality, used in (40), becomes unsharp. This point is readily verified for the estimator $\Delta^{\text{out}}_{N,\bar{\boldsymbol{\mu}}}$ by separate computation of the effectivities associated with the estimators $\Delta_N(\boldsymbol{\mu})$ and $\Delta_{\bar{\boldsymbol{\mu}}}(\boldsymbol{\mu})$ for the primal and dual problems, respectively, which are indeed close to unity (of course, the same argument works for the other estimators as well). For $N = 25$, we find

$$\max_{\boldsymbol{\mu} \in \Xi_{\text{test}}} \frac{\Delta_N(\boldsymbol{\mu})}{\|u_N(\boldsymbol{\mu}) - u^{\mathcal{N}}(\boldsymbol{\mu})\|_{\boldsymbol{\mu}}} \approx 2.68 \tag{77}$$

and (irrespective of N)

$$\max_{\boldsymbol{\mu}\in\Xi_{\text{test}}} \frac{\Delta_{\bar{\mu}}(\boldsymbol{\mu})}{\|\psi^{\mathcal{N}}(\bar{\boldsymbol{\mu}}) - \psi^{\mathcal{N}}(\boldsymbol{\mu})\|_{\boldsymbol{\mu}}} \approx 2.94. \tag{78}$$

Hence, we do have a quite sharp bound for the right hand side of (40) for all $\boldsymbol{\mu} \in \Xi_{\text{test}}$, and the unsharpness of the RB output error bound must be ascribed to the Cauchy-Schwarz inequality. Another implication of the sharpness of the individual error bounds is that our coercivity lower bound, $\alpha_{\text{LB}}(\boldsymbol{\mu})$, must be very sharp for all $\boldsymbol{\mu} \in \Xi_{\text{test}}$.

4.4 A note on a special compliant problem

Since the governing equation for our problem is the Laplace equation (58), the parameterised bilinear form $a(\cdot,\cdot;\boldsymbol{\mu})$ is symmetric for each $\boldsymbol{\mu} \in \mathcal{D}$, and the only term that enters on the right-hand-side in the weak formulation, e.g. (70), is the Dirichlet lifting term $-a(u^{\text{D}}, v; \boldsymbol{\mu})$. Now, in the very special case that we would like to evaluate the flux integral output over the same electrode on which a unity potential is imposed, we may choose $v^\star = u^{\text{D}}$ as the flux lifting function. In this case, our RB output of interest is $s_N(\boldsymbol{\mu}; u^{\text{D}}) = a(u_N(\boldsymbol{\mu}), u^{\text{D}}; \boldsymbol{\mu})$. With $e_N(\boldsymbol{\mu}) = u^{\mathcal{N}}(\boldsymbol{\mu}) - u_N(\boldsymbol{\mu})$, we get

$$\begin{aligned} |s^{\mathcal{N}}(\boldsymbol{\mu}) - s_N(\boldsymbol{\mu}; u^{\text{D}})| &= |a(e_N(\boldsymbol{\mu}), u^{\text{D}}; \boldsymbol{\mu})| \\ &= |a(u^{\text{D}}, e_N(\boldsymbol{\mu}); \boldsymbol{\mu})| \\ &= |a(u^{\mathcal{N}}(\boldsymbol{\mu}), e_N(\boldsymbol{\mu}); \boldsymbol{\mu})| \\ &= |a(e_N(\boldsymbol{\mu}), e_N(\boldsymbol{\mu}); \boldsymbol{\mu})| = \|e_N(\boldsymbol{\mu})\|^2_{\boldsymbol{\mu}}, \end{aligned} \tag{79}$$

where we use the symmetry of $a(\cdot,\cdot;\boldsymbol{\mu})$, then (60) and the fact that $e_N(\boldsymbol{\mu}) \in X^{\mathcal{N}}$, and finally again symmetry of $a(\cdot,\cdot;\boldsymbol{\mu})$ and Galerkin orthogonality. Hence, the RB output error converges quadratically with the energy-norm error without any simultaneous primal-dual treatment.

In the multi-electrode case, it is of little practical interest to evaluate the capacitance over the electrode with unity Dirichlet data, since this evaluation would only yield the *total* capacitance, as if we were to sum up the capacitances between the selected electrode and each of the other electrodes. However, for the sake of argument, suppose our system consists of only two electrodes. Then the exact output over one of the electrodes is equal to the exact output over the other, with a minus sign. We can thus choose to evaluate the output over the electrode with unity Dirichlet data (and multiply by (-1)).

We emphasise again that this compliant effect is restricted to the special case in which $f = 0$, the unity Dirichlet input electrode coincides with the output electrode and $a(\cdot,\cdot;\boldsymbol{\mu})$ is symmetric for each $\boldsymbol{\mu} \in \mathcal{D}$.

In [7], the numerical example discussed in Sections 4.1–4.3 is extended to incorporate three outputs (specifically, the capacitances between the south electrode, Γ_{south}, and each of the other electrodes, Γ_{east}, Γ_{north} and Γ_{west}). Also, several symmetries of the problem are exploited – which we have not done in

this paper for the sake of simplicity of exposition – and the empirical interpolation method is used in order to achieve an efficient offline-online decoupling of the RB computations. Finally, we also mention [20], in which a very similar electrostatics problem is solved with the *h-p* finite element method. As in our example, the outputs of interest are the capacitances corresponding to pairs of electrodes, and evaluation of the outputs both via a flux lifting function and by direct computation is considered.

5 Concluding Remarks

We have shown that the flux lifting function, which we call $v^\star$, should be chosen with care when evaluating flux integral outputs from reduced basis approximations. Our two different proposals for a "good" $v^\star$ have been seen to give better results (a smaller RB output error) than a naive $v^\star$ in a simple (Laplace equation) numerical example. In contrast, we note that the naive $v^\star$ would have performed equally well as the "good" ones within a standard finite element context. (In fact, the naive choice is convenient in terms of implementation, and is thus often used in practice for the FE method.)

In the case of many (flux integral) outputs of interest that are all functionals of the same RB solution, a standard primal-dual error reduction technique may become too expensive. In this case, choosing a good $v^\star$ is important to make sure that the RB (primal only) output error is not unnecessarily large.

Acknowledgements

We would like to thank Professor Anthony T. Patera of M.I.T., and Dr D.B.P. Huynh for the many helpful comments and suggestions recieved throughout the work on this paper. The work has been supported by the Norwegian University of Science and Technology.

References

[1] I. Babuška and A. Miller. The post-processing approach in the finite element method – part 1: Calculation of displacements, stresses and other higher derivatives of the displacements. *International journal for numerical methods in engineering*, 20:1085–1104, 1984.

[2] I. Babuška and M. Suri. The *p* and *h-p* versions of the finite element method, basic principles and properties. *SIAM Rev.*, 36(4):578–632, 1994.

[3] M. Barrault, Y. Maday, N. C. Nguyen, and A. T. Patera. An 'empirical interpolation' method: application to efficient reduced-basis discretization of partial differential equations. *C. R. Math. Acad. Sci. Paris*, 339(9):667–672, 2004.

[4] C. Bernardi and Y. Maday. Polynomial approximation of some singular functions. *Appl. Anal.*, 42(1):1–32, 1991.

[5] C. Bernardi and Y. Maday. Spectral methods. In *Handbook of numerical analysis, Vol. V*, Handb. Numer. Anal., V, pages 209–485. North-Holland, Amsterdam, 1997.

[6] G. F. Carey. Derivative calculation from finite element solutions. *Comput. Methods Appl. Mech. Engrg.*, 35(1):1–14, 1982.

[7] J. L. Eftang. Reduced basis methods for partial differential equations. Master's thesis, Norwegian University of Science and Technology, 2008.

[8] W. J. Gordon and C. A. Hall. Construction of curvilinear co-ordinate systems and applications to mesh generation. *Internat. J. Numer. Methods Engrg.*, 7:461–477, 1973.

[9] M. A. Grepl, Y. Maday, N. C. Nguyen, and A. T. Patera. Efficient reduced-basis treatment of nonaffine and nonlinear partial differential equations. *M2AN Math. Model. Numer. Anal.*, 41(3):575–605, 2007.

[10] P. M. Gresho, R. L. Lee, R. L. Sani, M. K. Maslanik, and B. E. Eaton. The consistent galerkin fem for computing derived boundary quantities in thermal and/or fluids problems. *International journal for numerical mehods in fluids*, 7:371–394, 1987.

[11] P. Grisvard. *Singularities in boundary value problems*, volume 22 of *Recherches en Mathématiques Appliquées [Research in Applied Mathematics]*. Masson, Paris, 1992.

[12] W. Gui and I. Babuška. The h, p and h-p versions of the finite element method in 1 dimension. I. The error analysis of the p-version. *Numer. Math.*, 49(6):577–612, 1986.

[13] A. E. Løvgren, Y. Maday, and E. M. Rønquist. A reduced basis element method for the steady Stokes problem. *M2AN Math. Model. Numer. Anal.*, 40(3):529–552, 2006.

[14] Y. Maday, N. C. Nguyen, A.T Patera, and G. S. H. Pau. A general multipurpose interpolation procedure: The magic points. *Communications in pure and applied mathematics*, 8:383–404, 2009.

[15] Y. Maday and A. T. Patera. Spectral element methods for the incompressible Navier-Stokes equations. In A.K. Noor and J.T. Oden, editors, *State of the art surveys in Computational Mechanics*, pages 71–143. American Society of Mechanical Engineers, 1989.

[16] N. C. Nguyen. *Reduced-Basis Approximations and* A Posteriori *Error Bounds for Nonaffine and Nonlinear Partial Differential Equations: Application to Inverse Analysis*. PhD thesis, Singapore-MIT Alliance, National University of Singapore, 2005.

[17] C. Prud'homme, D. V. Rovas, K. Veroy, L. Machiels, Y. Maday, A. T. Patera, and G. Turinici. Reliable real-time solution of parametrized partial differential equations: Reduced-basis output bound methods. *Journal of Fluids Engineering*, 124(1):70–80, 2002.

[18] A. Quarteroni and A. Valli. *Numerical approximation of partial differential equations*, volume 23 of *Springer Series in Computational Mathematics*. Springer-Verlag, Berlin, 1994.

[19] G. Rozza, D. B. P. Huynh, and A. T. Patera. Reduced basis approximation and a posteriori error estimation for affinely parametrized elliptic coercive partial differential equations. *Archives of Computational Methods in Engineering*, 15(3):229–275, 2008.

[20] B. A. Szabó. Solution of electrostatic problems by the p-version of the finite element method. *Comm. Appl. Numer. Methods*, 4(4):565–572, 1988.

[21] K. Veroy, C. Prud'homme, D. V. Rovas, and A. T. Patera. A posteriori error bounds for reduced-basis approximation of parametrized noncoercive and nonlinear elliptic partial differential equations. In *Proceedings of the 16th AIAA Computational Fluid Dynamics Conference*, 2003.